35th Annual International Conference of the IEEE EMBS
Osaka, Japan, 3 - 7 July, 2013

A New Quantitative Approach for Estimating Bone Cell Connections from Nano-CT Images

Pei Dong[1,2], Alexandra Pacureanu[1,2], Maria A. Zuluaga[1,2], Cécile Olivier[1,2], Frédérique Frouin[3], Quentin Grimal[4], Françoise Peyrin[1,2] *Member IEEE*

***Abstract*—Recent works highlighted the crucial role of the osteocyte system in bone fragility. The number of canaliculi of osteocyte lacuna (Lc.NCa) is an important parameter that reflects the functionality of bone tissue, but rarely reported due to the limitations of current microscopy techniques, and only assessed from 2D histology sections. Previously, we showed the Synchrotron Radiation nanotomography (SR-nanoCT) is a promising technique to image the 3D lacunar-canalicular network. Here we present, for the first time, an automatic method to quantify the connectivity of bone cells in 3D. After segmentation, our method first separates and labels each lacuna in the network. Then, by creating a bounding surface around lacuna, the Lc.NCa is calculated through estimating 3D topological parameters. The proposed method was successfully applied to a 3D SR-nanoCT image of cortical femoral bone. Statistical results on 165 lacunae are reported, showing a mean of 51, which is consistent with the literature.**

Index Terms— lacunar-canalicular network, automatic quantification, SR nano-CT, topological parameters, morphological operation

I. Introduction

Bone diseases significantly affect the quality of life around the world. However, bone fragility remains partially understood despite decades of research in this area. Recently, the crucial role of the osteocyte system at the cellular scale was highlighted [1]. The osteocyte system, which is composed of osteocytes communicating through dendrites, is essential in bone mechanosensing and bone mechanotransduction and is supposed to orchestrate bone adaptation [2]. This system is hosted in the lacunar-canalicular network (LCN), where osteocytes reside in ellipsoidal osteocyte lacunae and their dendritic cell processes are enclosed by canaliculi. It has been pointed out that the number of canaliculi (Lc.NCa) originating from each lacuna is an important indicator of the functionality of the bone tissue [3].

In previous works, we showed the feasibility of using synchrotron radiation nanotomography (SR nano-CT) to image the bone cellular network in 3D [4][5]. The SR-CT system installed at ESRF ID19 can provide images of bone tissue with a 3D isotropic spatial resolution of 300nm. The relatively large field of view (FOV) of about $600\mu m^3$ may include up to hundreds of osteocytes. Our previous works have been focused on the segmentation of the LCN from the reconstructed images [6][7][8]. After this step, quantification methods have to be developed. However, the current quantification tools are not adapted to the complexity of this network and to handle the large data set (2048^3) and the large population of lacuna and canaliculi. Therefore, due to the novelty of the images, new automated quantification methods are quite urgently needed.

Up to now, the assessment of the number of canaliculi emanating from lacuna is always based on manual analysis of 2D microscopic images. Remaggi measured it per 10µm of the lacuna perimeter in different bone species [9]. From these 2D measurements, Beno [10] et al. extrapolated the 3D total number of canaliculi by assuming an elliptical model of the lacuna. The authors reported a low and a high estimation of Lc.NCa in human bone, found between 18 and 106. However these results can be biased because the methods are based on an ideal model. Obviously, direct measurements on 3D images are necessary to get unbiased results on such strongly anisotropic structures. Experimental measurements of the 3D Lc.NCa have been reported by using confocal microscopy but calculation limited to 10 osteocytes [11]. Serial FIB/SEM was used to estimate a number of 78 canaliculi per in rat bone but this was extrapolated by counting only one third of the lacuna [12]. A common problem in these reports is that the quite narrow FOV cannot provide reliable biological results on the osteocyte network.

In this paper, we present a novel scheme to automatically quantify the Lc.NCa from 3D images on large FOV. This method is expected to yield unbiased results. Also, since this method is designed without manual interference, it can meet the requirement for quantification on the large population of cells.

II. Material And Methods

A. Samples preparation

The bone sample was extracted from the middle shaft of female femur (92 years old) obtained from a multi-organ collection. Sample was cut in nearly cuboid shape with the diagonals of transverse sections around 0.4mm and height about 1cm. The samples were collected following the procedure of the Human Ethics Committee of the "Centre du don des Corps" at the University Rene Descartes (Paris, France) and consistently with legal clauses stated in the French Code of Public Health.

[1] CREATIS, INSA-Lyon; Inserm, U1044; CNRS, UMR5220; Université de Lyon, 69621 Villeurbanne, France
[2] European Synchrotron Radiation Facility, X-Ray Imaging Group, 38043 Grenoble, France
[3] UMPC Univ Paris 6, UMRS 678, Laboratoire d'Imagerie Fonctionnelle, 75013 Paris, France
[4] UMPC Univ Paris 6, UMR 7623, Laboratoire d'Imagerie Paramétrique, 75013 Paris, France

B. Acquisition of SR-nanoCT images

Since the size of canaliculi is at the limit of the spatial resolution of the imaging system, it was necessary to optimize all its components [4]. To this aim, a 4.5 µm thick LSO scintillator coupled to a CCD camera was used. The voxel size was fixed to 300nm providing a FOV of about 600^3 µm^3. The X-ray beam energy was set to 18keV. During the scan, 2000 projections were recorded by rotating the samples around a vertical axis with a total angle of 180°. The scan time was around 30 minutes. After scanning, the 3D image was reconstructed using a standard filtered backprojection algorithm.

C. Segmentation of LCN

The segmentation of the LCN is quite challenging due to the limited spatial resolution compared to the size of canaliculi and low signal to noise ratio of the reconstructed image. Here, we applied our previous method to perform the LCN segmentation. First, we used a filter to enhance tubular structures based on Hessian analysis [13]. Then, a level set based method was applied to automatically perform the LCN segmentation [14]. Figure 1(b) shows the binaralized segmentation result of a region of interest (ROI) in a reconstructed slice (Figure 1(a)).

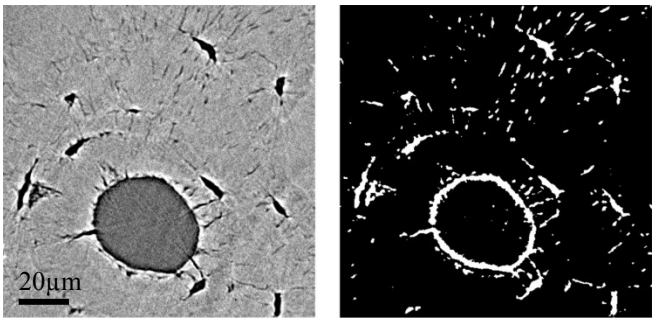

Figure 1. (a) ROI of 512×512 pixels in a single SR-nanoCT slice (voxel size 280nm) including a Haversian canal, lacunae and canaliculi. (b) The corresponding segmented slice (bone tissue in black and porosity in white)

D. Quantification of bone cell connections

Here, we propose an automated scheme for direct 3D measurement of the number of canaliculi for each lacuna, which is denoted (Lc.NCa). The proposed method first discriminates lacunae and canaliculi and then applies the counting process for each lacuna.

1) Discrimination of lacunae and canaliculi

The first step is to extract lacunae body from the networks and label them individually. Morphological operations [15] were used to separate lacunae and canaliculi. A 3D opening operation is performed to remove canaliculi. After that, the extracted lacunae are labeled by applying an efficient connected component analysis [16]. Figure 2 illustrates the original network around 3 lacunae as well as the labeled lacunae.

The segmented LCN image can be formalized as a union of all lacunae (L_i) with the set of canaliculi (C_i) associated to each lacuna:

$$LCN = \bigcup_{i=1}^{M}(L_i \cup C_i) \quad (1)$$

where M is the total number of lacunae in the image.

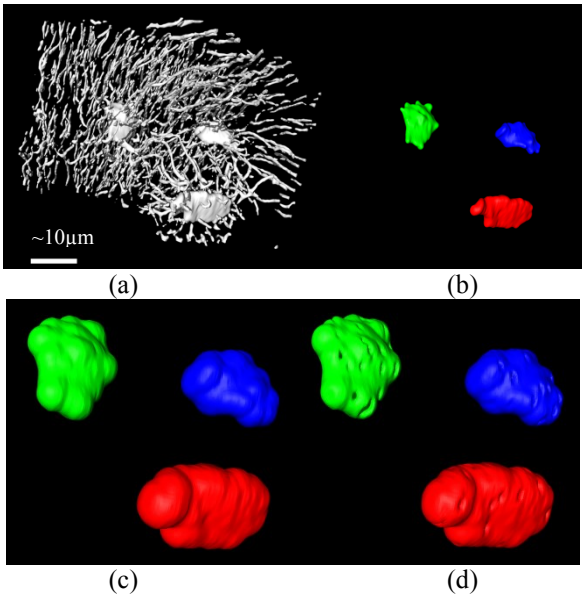

Figure 2. The quantification scheme on bone cell connections. (a) A 3D rendering on three interconnected lacunae and their connected canaliculi. (b) The extracted and labeled lacunae. Different colors represent the different labels. (c) Bounding surfaces of lacunae at certain distance away from the lacuna surfaces. The distances are same for the three labeled lacunae. (d) The bounding surfaces with holes. The number of holes on the surface equals to the number of canaliculi which penetrate the bounding surface.

2) Counting process

A counting process is then applied to each lacuna (L_i). Since previous observations suggested that the canaliculi may branch [3], we introduce a parameter *n* to define the distance from the lacuna surface where the number of canaliculi is calculated. First, we generate a bounding surface around a lacuna at the designated distance *n* (Figure 2(c)). It is denoted as $\partial_n L_i$. This surface is defined using the morphological derivative. It can be expressed as the subtraction between the *n*+1 and *n* times dilated lacuna:

$$\partial_n L_i = \oplus_{(n+1)} L_i - \oplus_n L_i \quad (2)$$

where $\oplus$ denotes dilation, *n* determines the distance between the lacuna surface and the bounding surface, the structuring element is a 3×3×3 cube.

After that, we create a special bounding surface with holes, which is denoted as $\mathcal{H}_n L_i$:

$$\mathcal{H}_n L_i = \partial_n L_i - (\partial_n L_i \cap C_i) \quad (3)$$

In this special object, which is illustrated in Figure 2(d), the number of holes is equal to the number of canaliculi which penetrate the bounding surface. The number of holes in a 3D object is related to the 3D Euler number, the number of the connected component and the number of cavity. Therefore, the number of canaliculi per lacuna can be calculated through topological parameters.

In theory, the 3D Euler number of an object in three-dimensional space can be expressed as:

$$\chi = \beta_0 - \beta_1 + \beta_2 \quad (4)$$

where β_0, β_1, β_2 are the Betti numbers representing respectively the number of connected components, the number of tunnels and the number of cavities in the object.

In practice, when the object is represented as a discrete set of voxels, the 3D Euler number can be calculated as [17]:

$$\chi = n_0 - n_1 + n_2 - n_3 \quad (5)$$

where n_0, n_1, n_2, and n_3 are respectively the number of vertices, edges, faces, and voxels.

According to this theory, the number of holes on the bounding surface can be calculated as:

$$\beta_1(\mathcal{H}_n L_i) = \beta_0(\mathcal{H}_n L_i) + \beta_2(\mathcal{H}_n L_i) - \chi(\mathcal{H}_n L_i) \quad (6)$$

By construction, $\mathcal{H}_n L_i$, $\beta_0(\mathcal{H}_n L_i)$ and $\beta_1(\mathcal{H}_n L_i)$ are equal to 1. Therefore, the number of canaliculi $\mathrm{Lc.NCa_i}$ for lacuna (L_i) at the distance n can be calculated as :

$$\mathrm{Lc.NCa_i} = \beta_1(\mathcal{H}_n L_i) = 2 - \chi(\mathcal{H}_n L_i) \quad (7)$$

where $\chi(\mathcal{H}_n L_i)$ is obtained from Equation (5).

III. Results

A. Validation on a single isolated lacuna

After testing the method on simple geometrical phantoms, the method was validated on a real binary SR phantom which was obtained by the manual segmentation of one isolated lacuna with all its canaliculi on an experimental SR nano-CT image, shown in Figure 3(a). The volume size is 149×149×85 voxels. Our method was tested on this phantom with two dilation parameters *n*, which equals to 1 and 15. The results of calculated numbers of canaliculi were respectively 22 and 32.

To prove the efficiency and accuracy of our method, a manual counting was performed. However, since it is difficult to achieve because of the complex structure of the canaliculi, this was done by a dedicated procedure. First, the canaliculi outside the bounding surface were extracted. Then, a connected component analysis was used and the labeled canaliculi were rendered in different colors using Avizo®. Figure 3(b) and (c) illustrate the rendering results for the two dilation parameters. The results of the manual check are in agreement with the results of our automated method.

The dilation parameter allows to evidence whether canaliculi branch or not. If the number of canaliculi calculated at two different bounding surfaces differs, as in this example, then some canaliculi branches.

B. Application to a large LCN network

The proposed method was applied to a large SR-nanoCT image acquired at the ESRF at a spatial resolution of 300nm. A Volume of Interest (VOI) made of 1600×1000×256 voxels was extracted from a $(2048)^3$ reconstructed volume. The VOI includes two osteons with over a hundred of lacunae.

The proposed method allowed estimating statistics on the number of connections per bone cells in a large field of view. During the process, 165 lacunae were successfully labeled in the segmented image, compared with a ground truth of 184 lacunae. The volume of the lacunae (Lc.V), the number of canaliculi per lacuna (Lc.NCa) and the Euler number χ of the bounding surface with holes were measured for all lacunae. We used a dilation parameter (n) equal to 15 corresponding to a distance of 4.2µm as on the isolated lacuna in validation, which is smaller than the half of the average distance between lacunae [11].

Table I shows the mean, standard deviation, minimum and maximum values of these characteristics from the 165 lacuna. The mean lacuna volume was 357.76 μm^3. The mean number of canaliculi per lacuna was found to be 50.99 with a standard deviation of 26.83 and a mode of 54. The Lc.NCa covers a wide range from 0 to 134. Figure 4 illustrates three typical lacunae with different numbers of canaliculi cropped from the segmented image.

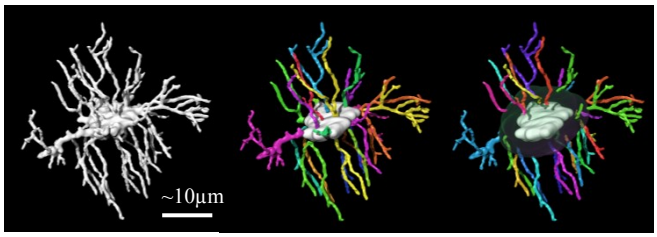

(a) (b) (c)

Figure 3. A manually segmented lacuna with fully connected canaliculi. Volume size is 149×149×85 voxels. Canaliculi are rendered in different colors to simplify the manual check. (a) 22 canaliculi are manually counted for dilation parameter n=1 (0.28µm away from the lacuna surface). (b) 32 canaliculi are manually counted for dilation parameter n=15 (4.2µm away from the lacuna surface).

TABLE I. Statistical results of the quantification method for 165 lacunae

***n*=15**	**Lc.NCa**	**Size (μm^3)**	**χ**
mean	50.99	357.76	-48.43
std	26.83	108.18	26.64
min	0	152.52	-132
max	134	878.72	2

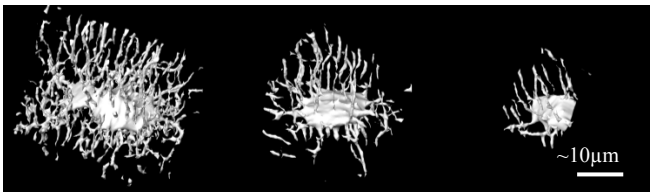

(a) (b) (c)

Figure 4. 3D renderings of three typical lacunae. (a) A lacuna whose canaliculi are calculated as 105 (b) A lacuna whose canaliculi are calculated as 54 (c) A lacuna whose canaliculi are calculated as 15

IV. Conclusion and Discussion

This work aims to provide new tools for the quantification of the bone cell network in 3D. In this paper, we proposed a new automatic technique to measure the numbers of connections departing from each bone cell from 3D SR-nanoCT images. The method was successfully tested on an isolated lacuna surrounded by all its canaliculi. Then, it was applied to a larger experimental image of human cortical femoral bone.

It is the first time that the number of canaliculi is measured automatically in 3D from 3D images having an isotropic spatial resolution. In this respect, SR nano-CT is an attractive new technique providing in one scan, a large number of cells. The traditional investigations on bone cell connection are based on 2D histological sections analyzed manually. Compared to the extrapolation of 2D measurements to 3D estimation, based on idealized lacuno-canalicular models, the present method does not require any model assumption. Thus it is expected to measure unbiased parameters. Since the method is fully automated, it could be applied to a human cortical bone with a large field of view including large population of cells.

The statistical result on 165 lacunae shows a feasibility of applying the counting method on large specimens for automatic quantification work. The mean number of canaliculi per lacuna was found as 51, when calculated at 4.2 μm away from the lacuna surface. The value of Lc.NCa varies between 0 and 134. The very small value might due to counting the partial lacuna lying on the boarder of the image, as shown in Figure 4(c). Although it is difficult to evaluate the accuracy of the result on the large image due to the enormous amount of manual segmentation work, the reported result is in agreement with the value estimated by Beno [10] who reported a mean number of 41 canaliculi per lacunae in human bone. Yet, this results need to be further confirmed in future work.

We may note that the results strongly rely on image segmentation which itself is dependent of the quality of the acquired image. Progresses should be done to improve image quality by optimizing the imaging setup and acquisition conditions. Progresses should also be done in the segmentation step to reduce noise and improve the connectivity of the lacuno-canalicular network.

In our method, the dilation parameter permitted to put in evidence the branching of canaliculi, nevertheless the results associated to various dilation parameters have to be further explored.

With the advantage of being 3D, automated and model independent, it is expected that the proposed method will open new perspectives for improving our knowledge on the LCN. Furthermore, future work will also be pursued to extract additional characteristics of the LCN, such as the canaliculi length and the canaliculi density per each lacuna.

ACKNOWLEDGEMENT

Images were acquired in the context of the ESRF LTP MD431. The authors thank Elodie Boller for help during experiment. They also acknowledge the support of the GdR STIC-Santé, and the ANR labex PRIMES (Physics radiobiology Medical imaging and Simulation) from the Université de Lyon, France

REFERENCES

[1] L. F. Bonewald, "The amazing osteocyte," J. Bone Miner. Res, vol. 26, no. 2, pp. 229–238, Feb. 2011.

[2] L. E. Lanyon, "Osteocytes, strain detection, bone modeling and remodeling," Calcif Tissue Int, vol. 53, no. S1, pp. S102–S107, Feb. 1993.

[3] M. L. Knothe Tate, J. R. Adamson, A. E. Tami, and T. W. Bauer, "The osteocyte," Int. J. Biochem. Cell Biol., vol. 36, no. 1, pp. 1–8, Jan. 2004.

[4] A. Pacureanu, M. Langer, E. Boller, P. Tafforeau, and F. Peyrin, "Nanoscale imaging of the bone cell network with synchrotron X-ray tomography: optimization of acquisition setup," Med Phys, vol. 39, no. 4, pp. 2229–2238, Apr. 2012.

[5] M. Langer, A. Pacureanu, H. Suhonen, Q. Grimal, P. Cloetens, and F. Peyrin, "X-Ray Phase Nanotomography Resolves the 3D Human Bone Ultrastructure," PLoS ONE, vol. 7, no. 8, p. e35691, Aug. 2012.

[6] A. Pacureanu, A. Larrue, Z. Peter, and F. Peyrin, "3D non-linear enhancement of tubular microscopic bone porosities," in 2009 IEEE International Symposium on Biomedical Imaging: From Nano to Macro, Boston, MA, USA, 2009, pp. 602–605.

[7] A. Pacureanu, C. Revol-Muller, J. Rose, M. S. Ruiz, and F. Peyrin, "Vesselness-guided variational segmentation of cellular networks from 3D micro-CT," in 2010 IEEE International Symposium on Biomedical Imaging: From Nano to Macro, 2010, pp. 912 –915.

[8] A. Pacureanu, J. Rollet, C. Revol-Muller, V. Buzuloiu, M. Langer, and F. Peyrin, "Segmentation of 3D Celluar Networks from SR-MICRO-CT Images," in 2011 IEEE International Symposium on Biomedical Imaging: From Nano to Macro, Chicago, USA, 2011, pp. 1970–1973.

[9] F. Remaggi, V. Canè, C. Palumbo, and M. Ferretti, "Histomorphometric study on the osteocyte lacuno-canalicular network in animals of different species. I. Woven-fibered and parallel-fibered bones," Ital J Anat Embryol, vol. 103, no. 4, pp. 145–155, Dec. 1998.

[10] T. Beno, Y.-J. Yoon, S. C. Cowin, and S. P. Fritton, "Estimation of bone permeability using accurate microstructural measurements," Journal of Biomechanics, vol. 39, no. 13, pp. 2378–2387, 2006.

[11] Y. Sugawara, H. Kamioka, T. Honjo, K. Tezuka, and T. Takano-Yamamoto, "Three-dimensional reconstruction of chick calvarial osteocytes and their cell processes using confocal microscopy," Bone, vol. 36, no. 5, pp. 877–883, May 2005.

[12] P. Schneider, M. Meier, R. Wepf, and R. Müller, "Serial FIB/SEM imaging for quantitative 3D assessment of the osteocyte lacuno-canalicular network," Bone, Apr. 2011.

[13] A. Pacureanu, A. Larrue, Z. Peter, and F. Peyrin, "3D non-linear enhancement of tubular microscopic bone porosities," in IEEE International Symposium on Biomedical Imaging: From Nano to Macro, 2009. ISBI '09, 2009, pp. 602 –605.

[14] A. Pacureanu, J. Rollet, C. Revol-Muller, V. Buzuloiu, M. Langer, and F. Peyrin, "Segmentation of 3D cellular networks from SR-micro-CT images," in 2011 IEEE International Symposium on Biomedical Imaging: From Nano to Macro, 2011, pp. 1970 –1973.

[15] J. Serra, Image analysis and mathematical morphology. Academic Press, 1982.

[16] J. Hoshen and R. Kopelman, "Percolation and cluster distribution. I. Cluster multiple labeling technique and critical concentration algorithm," Phys. Rev. B, vol. 14, no. 8, p. 3438, Oct. 1976.

[17] J. Toriwaki and H. Yoshida, Fundamentals of three-dimensional digital image processing. Springer-Verlag New York Inc, 2009.

[18] A. Pacureanu, M. Langer, E. Boller, P. Tafforeau, and F. Peyrin, "Nanoscale imaging of the bone cell network with synchrotron X-ray tomography: optimization of acquisition setup," Med Phys, vol. 39, no. 4, pp. 2229–2238, Apr. 2012.